

Article

Understanding the Catalytic Effect on the CO₂ Regeneration Performance of Amine Aqueous Solutions

Ke Li ^{1,2}, Yuhang Shen ¹, Teng Shen ¹, Zhijun He ², Rui Zhou ¹, Zhouxiang Li ², Youhong Xiao ³, Euiseok Hong ⁴ and Haoran Yang ^{2,*} 

¹ Shanghai Qiya Environmental Technology Co., Ltd., Shanghai 200011, China; like@smderi.com.cn (K.L.); shenyuhang@smderi.com.cn (Y.S.); shenteng@smderi.com.cn (T.S.); zhourui@smderi.com.cn (R.Z.)

² Shanghai Marine Diesel Engine Research Institute, Shanghai 201108, China; hezhijun@smderi.com.cn (Z.H.); lizhouxiang@smderi.com.cn (Z.L.)

³ College of Power and Energy Engineering, Harbin Engineering University, Harbin 150009, China; xiaoyouhong@hrbeu.edu.cn

⁴ JNE SYSTECH Co., Ltd., Seoul 06661, Republic of Korea; eshong@jneworks.com

* Correspondence: yanghaoran@smderi.com.cn

Abstract: To address the high energy consumption of the carbon capture and storage process in the shipping industry, the effects of several commonly used commercial catalysts, such as HZSM-5-25, γ -Al₂O₃, and SiO₂, as well as a self-prepared catalyst, Zr-HZSM-5-25, on the regeneration of MEA solution and MEA + MDEA mixed solution were investigated in this paper. The results showed that Zr-HZSM-5-25 had the best catalytic effect on the regeneration process of the MEA aqueous solution, which could increase the instantaneous maximum CO₂ regeneration rate of the MEA-rich solution by about 8.25% and the average regeneration rate by about 5.28%. For the MEA + MDEA mixed solution, the reaction between tertiary amine MDEA and CO₂ produced a large amount of HCO₃⁻ in the reaction system, which could accelerate the release of CO₂ to a large extent, which resulted in the catalytic effect of the Zr-HZSM-5-25 catalyst on the regeneration process of the mixed amine solution being significantly lower than that on the single MEA solution, with an increase of 4.91% in the instantaneous maximum regeneration rate. This instantaneous maximum regeneration rate was only increased by 4.91%. While Zr-HZSM-5-25 showed a better performance in the bench-scale test, it reduced CO₂ regeneration energy consumption by 7.3%.

Keywords: carbon capture; regeneration energy consumption; catalysts



Citation: Li, K.; Shen, Y.; Shen, T.; He, Z.; Zhou, R.; Li, Z.; Xiao, Y.; Hong, E.; Yang, H. Understanding the Catalytic Effect on the CO₂ Regeneration Performance of Amine Aqueous Solutions. *Processes* **2024**, *12*, 1801. <https://doi.org/10.3390/pr12091801>

Academic Editors: Paola Ammendola and Federica Raganati

Received: 16 July 2024

Revised: 12 August 2024

Accepted: 16 August 2024

Published: 24 August 2024



Copyright: © 2024 by the authors. Licensee MDPI, Basel, Switzerland. This article is an open access article distributed under the terms and conditions of the Creative Commons Attribution (CC BY) license (<https://creativecommons.org/licenses/by/4.0/>).

1. Introduction

CO₂ emissions caused by fossil fuel use have now become a global issue [1], especially in the shipping industry, which accounts for 90% of global trade [2]. Onboard Carbon Capture and Storage (OCCS) technology can achieve large-scale CO₂ capture and storage, considered an important technical means to control global greenhouse gas emissions and meet the CO₂ emission reduction plan of the International Maritime Organization (IMO) [3,4]. Post-combustion chemical absorption is a CO₂ capture technology that has been applied in many other industries, such as refineries [5–7], pulp and paper industries [8], steel mills [9], coal gasification [10], and fossil fuel power plants [11,12]. Monoethanolamine (MEA) solution is widely used as a chemical absorbent in industrial CCS due to its low price, excellent CO₂ absorption properties, and other advantages [13,14]. The reaction heat between MEA and CO₂ ranges between 80 and 100 kJ/mol [15], which allows MEA to absorb CO₂ spontaneously. Conversely, the MEA solution requires a high regeneration temperature and regeneration energy consumption during the CO₂ regeneration process [16,17]. In traditional CCS technology, the temperature of the CO₂ regeneration process usually needs to reach higher than 100 °C to achieve a higher CO₂ regeneration rate and high regeneration temperature [18,19]. Since water accounts for 60–80 wt.% of the solution, it is

likely to evaporate, resulting in a large loss of secondary steam [20]. On vessels, additional power can only be generated by burning more fuels, which leads to more CO₂ emissions. Therefore, if it is possible to desorb CO₂ at a temperature lower than 100 °C in an OCCS system, the latent heat loss during the regeneration process will be greatly reduced, and the regeneration energy consumption of the system will be reduced [21,22].

In recent years, many scholars have investigated mixed amine and solid catalyst systems to address the high regeneration energy consumption in CCS processes [23–25]. Methyl diethanol amine (MDEA) has become a favored absorbent in the new low-energy-consumption CCS process due to its high CO₂ load, low corrosion, low reaction heat, and good regeneration performance. However, due to the low absorption rate of MDEA, mixed amine systems are usually adopted, combining compounds like MEA, MDEA, PZ, and DEA. Research suggests that mixed amines have a higher CO₂ load, better absorption reaction kinetics, and lower energy consumption than single-compound amines. For these mixed amine systems, researchers have carried out extensive studies: Idem et al. [26] compared the absorption and regeneration performance between MEA aqueous solution and MEA + MDEA aqueous solution and pointed out that the mixed amine solution could maintain the same absorption performance as the single MEA. In addition, researchers have used catalysts to reduce the energy consumption of the regeneration reaction, thus decreasing the regeneration temperature and reducing the regeneration energy consumption. Idem et al. [27] and Shi et al. [21] initially proposed the use of Bronsted-proton donor acid (HZSM-5) and Lewis-electron acceptor acid (γ -Al₂O₃) to reduce the activation energy of the reaction between protonated amine deprotonation and carbamate carbon dioxide release, thus accelerating the reaction rate. Wang et al. [28] studied several different HZSM-5 catalysts in intermittent and continuous regeneration tests, and the results showed that HZSM-5 has strong surface acidity, with the acidic center of the particle surface adsorbing more amines. As a result, the CO₂ regeneration promotion effect was more obvious. They also added nanoparticles of SiO₂, TiO₂, and Al₂O₃ to the MEA-rich solution. The regeneration rate was increased by 18–40% compared to the solutions without nanoparticles, and they suggested that the nanoparticles provided more bubble nucleation sites and promoted CO₂ regeneration. Zhang et al. [29] reported a novel acid–base bifunctional catalyst system, MCM-41, which is a mesoporous zeolite with a large specific surface area and low Bronsted acid site density. By modifying MCM-41 with three different metals (Fe, Al, Mo), the Bronsted and Lewis acidic sites and the Lewis alkaline sites on the surface of the catalyst were effectively increased. The results showed that the three catalysts could accelerate the regeneration process of MEA, and the MCM-41 (MFe) catalyst modified by Fe₂O₃ showed good catalytic performance. Compared with the catalyst-free operation, the addition of Fe greatly improved the regeneration performance of CO₂, reaching 206.3–337.1%.

These catalyst-focused studies are expected to develop rapidly in the coming years and be tested on a pilot-scale bench where they can be extensively explored. The goal is to achieve industrial-scale applications that will greatly reduce the heat load of CO₂ in the regeneration process and effectively reduce the size of the regeneration tower [30–32].

Although considerable research has been conducted on the properties of mixed amine solutions and the catalytic regeneration of amine solutions, there is no detailed assessment of the catalytic regeneration of mixed amine solutions. To realize the practical application of these technologies in engineering projects, understanding the basic dynamics of CO₂ gas with single amines and mixed amines during the reaction process is crucial for the effective design of absorption–regeneration systems. In this work, we compare several commonly used commercial catalysts HZSM-5-25, γ -Al₂O₃, and SiO₂, as well as a self-prepared catalyst Zr-HZSM-5-25, in the regeneration process of the MEA/MDEA solutions in the temperature range of 55 °C–85 °C using a regeneration test device and a bench-scale test platform.

2. Materials and Methods

In previous research, many catalysts have been introduced to enhance the CO₂ regeneration performance and reduce the regeneration energy consumption in the regeneration process of amine solutions. In this study, four catalyst materials are investigated, Zr-HZSM-5-25, HZSM-5-25, γ-Al₂O₃, and SiO₂. HZSM-5-25, γ-Al₂O₃, and SiO₂ are widely used by other researchers and purchased from manufacturers directly. The Zr-HZSM-5-25 catalyst is prepared in the laboratory. The solid acid catalyst materials are prepared by the ion exchange method. Taking Zr-HZSM-5-25, a group of solid acid materials with the highest catalytic performance in this study, 5 g of the Zr(SO₄)₂ is weighed and added into 100 mL of the deionized water and stirred until completely dissolved. And 10 g of the HZSM-5-25 molecular sieve is added at a uniform rate and stirred until the mixed solution is free of the precipitation. Then, the water is evaporated to dryness. The dried precursor is calcined in a tube furnace (programmed to increase the temperature by 5 °C/min, raised to 500 °C, and maintained there for 5 h) to obtain solid acid catalyst particles, which are then ground to powder form to produce the Zr-HZSM-5-25 bimetallic solid acid catalysts. The relevant physicochemical properties of these catalysts are shown in Table 1.

Table 1. Test products.

Item	Molecular Formula	Specifications	Formula Weight	Manufacturer
MEA	H ₂ N(CH ₂) ₂ OH	99%	61.09	Maclin, Shanghai, China
MDEA	CH ₃ N(CH ₂ CH ₂ OH) ₂	99%	119.16	Maclin, Shanghai, China
Zirconium sulfate	Zr(SO ₄) ₂	AR	283.35	Maclin, Shanghai, China
HZSM-5-25		AR	-	Nankai, Tianjin, China
γ-Al ₂ O ₃	Al ₂ O ₃	AR	101.96	Nankai, Tianjin, China
Silica	SiO ₂	AR	60.08	Nankai, Tianjin, China
Carbon dioxide	CO ₂	99%	44	Peric, Handan, China

The regeneration device, as depicted in Figure 1, consists of several essential components: a magnetic heating water bath, a float flow meter, a condensate pipe, a three-port flask, a nitrogen bottle, an exhaust gas analyzer, and a thermocouple. Regeneration tests are performed using the three-port flask, which is equipped with a condensate pipe and a thermocouple and is operated at atmospheric pressure. During the test, the solution is heated with the water bath, while the thermocouple provides real-time temperature monitoring. The condensate pipe enables the condensation and recovery of the evaporated solution, thus preventing the loss of the amine solution. Finally, the gas collected by the condenser tube is analyzed for concentration using the gas analyzer.

For the rich solution preparation process, 500 mL of 30 wt.% amine solutions is filled in a beaker and the pure CO₂ is passed into it for 30 min. In each group of regeneration tests, 30 mL of amine-rich solution is added to three-port flasks, and the solid catalysts addition amount is 2 g per experiment. The final regeneration temperature is controlled at about 85 °C through the water bath. When the solution temperature reaches 55 °C, the timing starting point and the changes in solution temperature and CO₂ concentration at the outlet of the condenser pipe per minute are recorded.

To further investigate the catalyst performance, a bench-scale CO₂ continuous absorption and regeneration platform is designed and constructed, as shown in Figure 2. The gas treatment capacity of the test platform is 3–36 m³/h. All the equipment and piping are made of 316 L stainless steel. The inner diameter of the absorption tower is 0.085 m and the height of the tower is 2.5 m. The absorption tower is packed with 5 × 5 Dixon rings. The inner diameter of the regeneration tower is 0.065 m and the height of the tower is 2.5 m. The regeneration tower is packed with 5 × 5 Dixon rings and it can replace the packing with catalyst material.

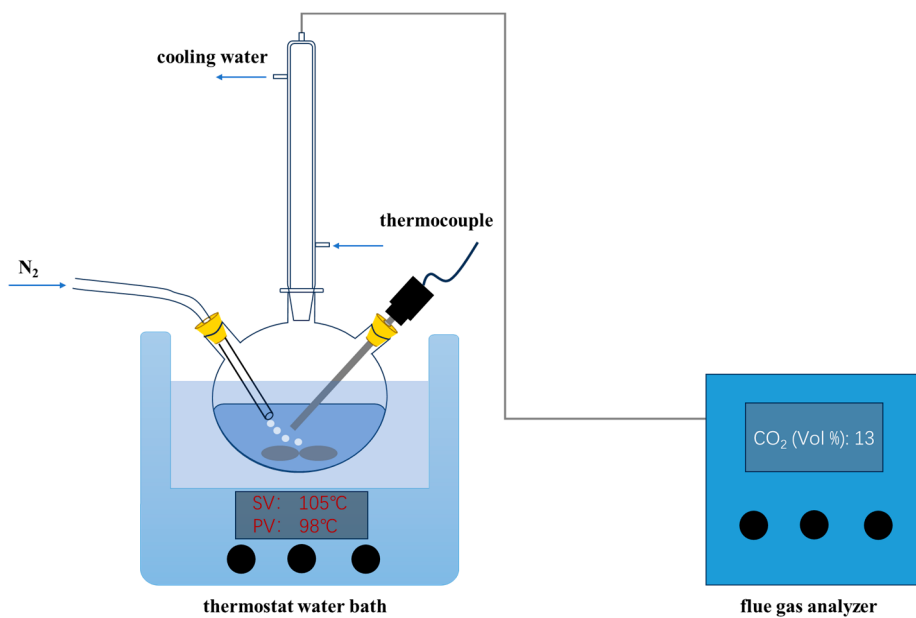


Figure 1. The regeneration device.



Figure 2. The CO₂ continuous absorption and regeneration platform.

According to the composition of the vessels' exhaust gas, the platform is equipped with a mixing gas system for the test, with a CO₂ content of 5% (v/v). The background gas (95% N₂% and 5% O₂) from a N₂ gas generator and the pure CO₂ gas from the purchased CO₂ cylinder are introduced into the gas buffer tank. The background gas flow and CO₂ gas flow go through the pressure reducing valves and flow meters, before mixing in the buffer tank. After mixing uniformly, the mixing gas enters the absorption tower from the bottom. And then the CO₂ is absorbed by the amine solution and the exhaust gas is discharged from the top of the tower. The rich amine solution after absorbing CO₂ passes through the heat exchanger to recover heat and then goes to the regeneration tower. The desorbed CO₂ together with water vapor is cooled and separated and the water is removed

to obtain the product CO_2 . The condensate from the regeneration gas is condensed and separated into the regeneration tower. The rich solution enters the regeneration tower from the top and then the reboiler to further regenerate the CO_2 . The catalysts are fixed in the middle of the regeneration tower by some support materials. After that, the lean amine solution flows out from the bottom of the regeneration tower. It is pumped to the water cooler and cooled in the absorption tower after going through the lean-rich solution heat exchanger. The reboiler is heated by electricity. The platform simulates the process and operating parameters of industrial devices, which can directly evaluate the CO_2 absorption rate, absorption capacity, regeneration performance, and regeneration energy consumption of the amine solution in a continuous dynamic state.

3. Results and Discussion

3.1. Theoretical Analysis

3.1.1. Chemical Reaction Mechanism

According to the zwitterion mechanism proposed by Caplow et al. [33], the absorption reaction process of the MEA and CO_2 produces zwitterion first, further releases the protons, and produces the carbamate (MEACOO^-) and protonation amine (MEAH^+). The reaction formulas are as follows:

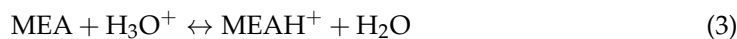
Zwitterion production:



Carbamate generation:

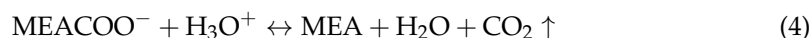


Protonated amine generation:

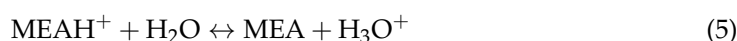


The amine regeneration process can be divided into two main steps [34]: the carbamate resolution and the protonated amines. The reaction formulas are as follows:

Carbamate decomposition:



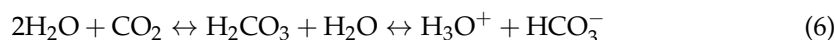
The protonated amine is deprotonated:



According to the reaction step described above, due to the high alkalinity of the amine solution, reaction (5) transferring the proton from MEAH^+ to H_2O has a high energy barrier and the decomposition of carbamate in the reaction (4) is a strong endothermic reaction with a high demand for the heat load.

Therefore, the CO_2 regeneration rate can be effectively increased by adding an appropriate amount of solid acid catalysts to the solution. Due to the fact that the acidic sites on the surface of the added solid acid catalyst can accelerate the reaction by providing protons to directly participate in the process of reaction (4), acid catalysts reduce the activation energy required for the regeneration [34].

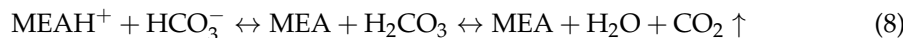
In addition, adding MDEA will also increase the CO_2 regeneration rate. According to the alkali catalytic hydration reaction mechanism, due to the lack of hydrogen atoms in the amine functional group, the carbamate cannot be produced during the reaction with CO_2 , but the bicarbonate can be formed [35]. The reaction formula is as follows:



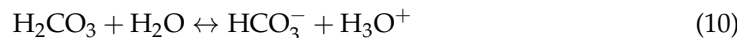
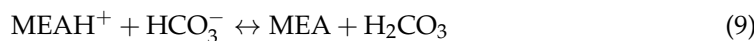


There are two favorable factors for the CO_2 regeneration of HCO_3^- in solution. Firstly, the HCO_3^- can act as a proton receptor, accepting the protonated amine released into H_2CO_3 , but the H_2CO_3 heating process can cause the direct decomposition into H_2O and CO_2 . Secondly, the HCO_3^- can be seen as a catalyst for the protonated amine decomposition into two compounds with the lower activation energy and provide protons for reaction (4): carbamate decomposition. Since the alkalinity of HCO_3^- is between amine and H_2O , the proton transfer from MEAH^+ to HCO_3^- and then to water requires a lower activation energy than the direct transfer to water [36]. The reaction formula is as follows:

HCO_3^- as a reactant:



HCO_3^- as a catalyst:



3.1.2. Calculation Method

CO_2 Absorption Efficiency

The absorption efficiency η is often used during chemical tests to indicate the degree of gas absorption after it has been scrubbed through a tower absorption plant. It can be expressed as

$$\eta = \frac{x_1 - x_2}{x_1} \times 100\% \quad (11)$$

The CO_2 volume fractions are measured during tests, also known as molar fractions. The equation for the conversion relationship between them is

$$X = \frac{x}{1-x} \quad (12)$$

Equations (11) and (12) give the CO_2 absorption efficiency as

$$\eta = \frac{x_1 - x_2}{x_1(1-x_2)} \times 100\% \quad (13)$$

where x_1 is the volume fraction of the CO_2 inlet to the absorption tower and x_2 is the volume fraction of the CO_2 outlet to the absorption tower.

Energy Consumption for Regeneration

The energy consumption for regeneration can be calculated by the amount of CO_2 captured and the energy consumption. The amount of CO_2 captured can be considered the amount of CO_2 regeneration under stable running conditions. So, the amount of CO_2 captured can be determined from the CO_2 absorption efficiency and CO_2 mass flow rate. And then, the regeneration energy consumption can be determined from the power consumed by the reboiler. It can be expressed as follows:

$$q_{\text{reg}} = \frac{Q_{\text{reg}}}{m_{\text{CO}_2}} \quad (14)$$

where q_{reg} is the CO_2 regeneration energy consumption, Q_{reg} is the energy consumption, and m_{CO_2} is the amount of CO_2 capture.

3.2. Characterization of Catalysts

The surface properties of four solid acid catalysts are investigated: Zr-HZSM-5-25, HZSM-5-25, γ -Al₂O₃, and SiO₂. The results are shown in Table 2. The total acid quantity of these four catalysts increases in the following order: Zr-HZSM-5-25 > HZSM-5-25 >

$\gamma\text{-Al}_2\text{O}_3 > \text{SiO}_2$. The BET results of the four catalysts increases in the following order: $\text{SiO}_2 > \text{Zr-HZSM-5-25} > \text{HZSM-5-25} > \gamma\text{-Al}_2\text{O}_3$.

Table 2. The surface properties of catalysts.

Catalyst	Total Acid Quantity (mmol/g)	BET Specific Area (m ² /g)	Average Pore Diameter (nm)	Pore Volume (cm ³ /g)
Zr-HZSM-5-25	2.44	380	0.89	0.34
HZSM-5-25	2.34	365	0.8	0.24
$\gamma\text{-Al}_2\text{O}_3$	0.385	234.6	4.51	0.37
SiO_2	0	450	6.05	0.43

The XRD patterns of the Zr-HZSM-5-25 and HZSM-5-25 catalysts are shown in Figure 3. It is clear that the XRD peaks of the Zr-HZSM-5-25 and HZSM-5-25 catalysts show similarity and the diffraction peaks of the Zr species are not detected in the XRD spectra. These results prove that the Zr modification does not have any effect on the molecular sieve's backbone structure and the Zr is highly dispersed on HZSM-5-25 molecular sieves.

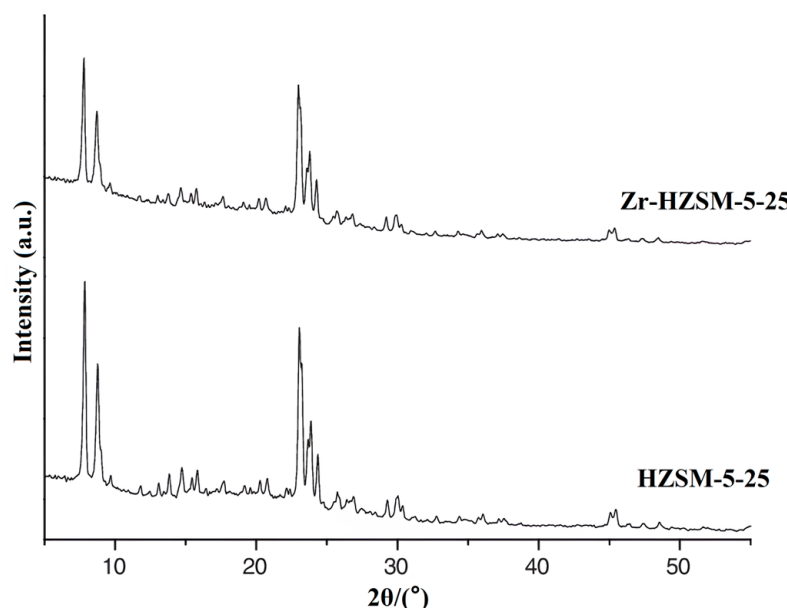


Figure 3. The XRD patterns of Zr-HZSM-5-25 and HZSM-5-25 catalysts.

The surface acidity of the Zr-HZSM-5-25 and HZSM-5-25 catalysts is determined by NH₃-TPD. The obtained NH₃ desorption patterns are shown in Figure 4. Two obvious peaks can be seen for the Zr-HZSM-5-25 and HZSM-5-25 catalysts. The first peak appearing at low temperature around 223 °C indicates the medium-strong acidic sites and the other at a high temperature around 420 °C is ascribed to the strong acidic sites. In addition, the NH₃ uptake of the Zr-HZSM-5-25 catalyst is higher than that of the HZSM-5-25 catalyst at 223 °C and 420 °C, which suggests that the Zr-HZSM-5-25 catalyst has more strong acid sites than the HZSM-5-25 catalyst. Thus, the modification of HZSM-5 with Zr increases its total acid sites.

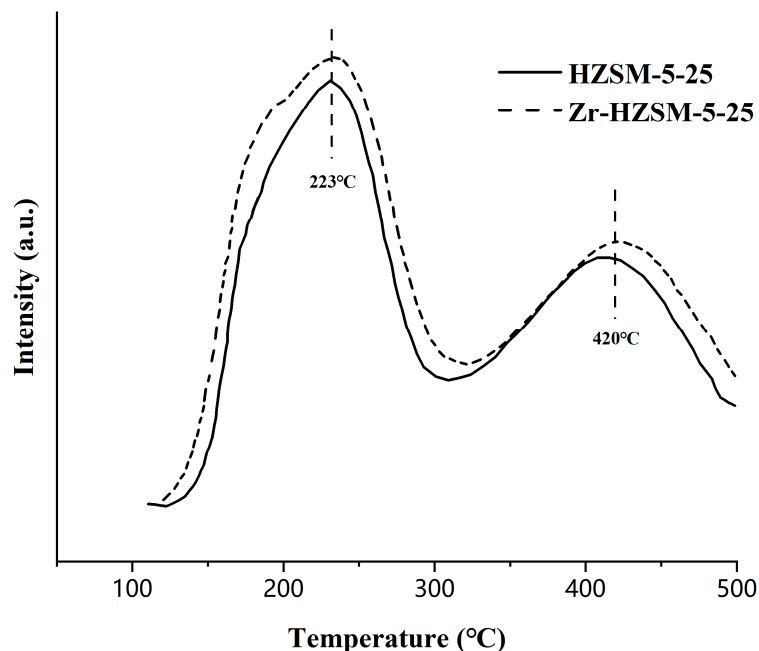


Figure 4. The $\text{NH}_3\text{-TPD}$ acidity profiles of the Zr-HZSM-5-25 and HZSM-5-25 catalysts.

3.3. Catalytic Regeneration Test of the MEA Solution

To study the effect of the catalyst surface characteristics on the rich solution during the regeneration process, the regeneration test is carried out in a reactor as shown in Figure 1.

Figure 5 shows the instantaneous CO_2 regeneration rate profile over a 35 min period. It is found that a high regeneration rate is maintained for the first 35 min. The catalyst addition can accelerate the regeneration rate of CO_2 to some extent. For the peak rate of CO_2 regeneration, the catalytic effect of the catalyst increases in the following order: Zr-HZSM-5-25 > HZSM-5-25 > $\gamma\text{-Al}_2\text{O}_3$ > blank > SiO_2 . The maximum regeneration rate increases by about 8.25%, which is consistent with the surface acid strength law of the catalyst used for testing. In addition, it is not difficult to find that the $\gamma\text{-Al}_2\text{O}_3$ and SiO_2 do not show an obvious catalytic effect in the heating stage of the solution. On the contrary, as the regeneration proceeds for a period of time, the temperature of the solution stabilizes gradually, and the catalytic effect of these two catalysts begins to show. For the $\gamma\text{-Al}_2\text{O}_3$ catalyst, as the carbon load of the solution decreases, the value of the solution pH increases gradually. This results in the $\gamma\text{-Al}_2\text{O}_3$ surface becoming negatively charged and AlO_2^- being produced as a Lewis basic site. The AlO_2^- promotes the deprotonation of protonated amine and provides a large number of protons for the decomposition process of carbamate, accelerating the regeneration process of CO_2 . In addition, the hydroxyl group in $\gamma\text{-Al}_2\text{O}_3$ can also produce HCO_3^- , with the free CO_2 in the low- CO_2 loading solution. The HCO_3^- in solution can also accelerate the regeneration process of CO_2 (reaction formulas (8)–(10)). Therefore, the CO_2 is released in the solution and the $\gamma\text{-Al}_2\text{O}_3$ catalyst can still maintain a relatively obvious catalytic effect. For the catalyst SiO_2 , although there is no acid site on the surface, its large specific surface area can provide more bubble nucleation sites for the regeneration of MEA solution under high-temperature conditions and enhance the overall mass transfer effect. The SiO_2 addition increases the effective interface area of air and liquid and accelerates the regeneration rate of CO_2 .

As shown in Figure 6, the temperature rise curve varies for each test, which may affect the instantaneous regeneration rate of CO_2 . So, the CO_2 regeneration amount results are shown in Figure 7. The calculated average CO_2 regeneration rate is shown in Table 3. The average CO_2 regeneration rate increases in the following order, Zr-HZSM-5-25 > $\gamma\text{-Al}_2\text{O}_3$ > HZSM-5-25 > SiO_2 > Blank, and the average rates of the CO_2 regeneration are 5.28%, 3.11%, 2.89%, and 2.6%, respectively. The modified catalyst Zr-HZSM-5-25 shows the most significant promoting effect on the CO_2 regeneration process, which is attributed to

the strong Bronsted acidic sites on the surface of the catalyst, which can directly provide protons for reaction (4) and accelerate the whole regeneration process. For the $\gamma\text{-Al}_2\text{O}_3$ catalyst, it mainly benefits from the AlO_2^- generated during the low carbon loading of the amine solution. The AlO_2^- works as a Lewis basic site to promote the protonated amine deprotonation in reaction (5) and provides a large number of protons for the decomposition process of carbamate in reaction (4), accelerating the regeneration of CO_2 . While the SiO_2 catalyst does not possess acidity, there is also non-homogeneous bubble nucleation, which has less promotion in the regeneration process [28,34].

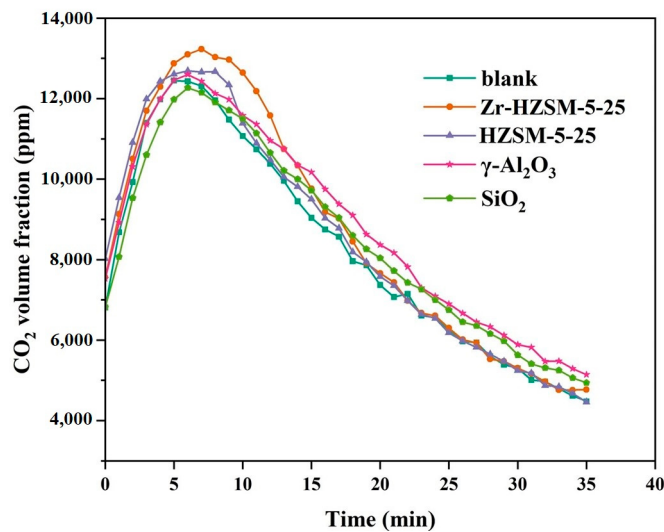


Figure 5. The CO_2 regeneration rate of the MEA solution (measured by the equipment shown in Figure 1).

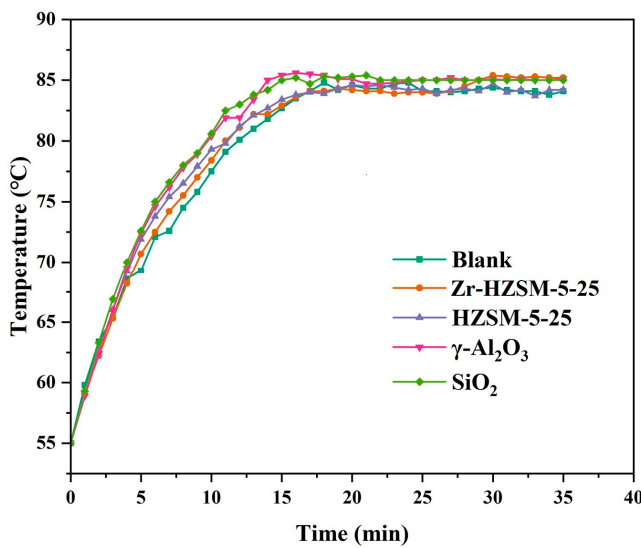


Figure 6. The temperature change curve (measured by the equipment shown in Figure 1).

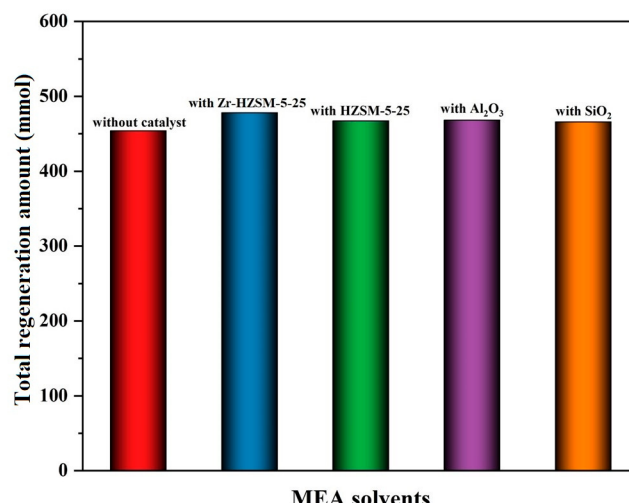


Figure 7. The total CO₂ regeneration amount of the MEA solution (measured by the equipment shown in Figure 1).

Table 3. The average regeneration rate of the MEA solution (measured by the equipment shown in Figure 1).

	Blank	Zr-HZSM-5-25	HZSM-5-25	γ -Al ₂ O ₃	SiO ₂
The average regeneration rate (mmol/min)	12.98	13.66	13.35	13.38	13.31
The promotion effect (%)	—	5.28	2.89	3.11	2.6

3.4. Catalytic Test of Mixed Amine Solutions

According to the results of the previous section, it is found that the Zr-HZSM-5-25 catalyst has the best catalytic performance for MEA solution regeneration among all four catalysts. To further investigate the catalyst's effect on the mixed amine solution, 500 mL of 30 wt% mixed amine solution is prepared and the rich solution is treated by pure CO₂ for 30 min. The regeneration test procedures and data analysis methods remain consistent with those previously described.

As shown in Figure 8, it is found that under the same test conditions, by adding a small amount of MDEA solution to the MEA solution, the improvement effect of the CO₂ regeneration peak rate is about 9.79%, while the improvement effect of the average regeneration rate is about 4.34%, as shown in Figure 9. From reaction (6) and reaction (7), it can be seen that the addition of the MDEA system produces a higher concentration of HCO₃⁻ groups after reaction with CO₂. The presence of HCO₃⁻ reduces the activation energy of the MEAH⁺ deprotonation process, improves the increase in MEAH⁺ deprotonation rate, and accelerates the rate of MEACOO⁻-decomposition-releasing CO₂. The reaction with MEAH⁺ causes H₂CO₃ heat decomposition to H₂O and CO₂.

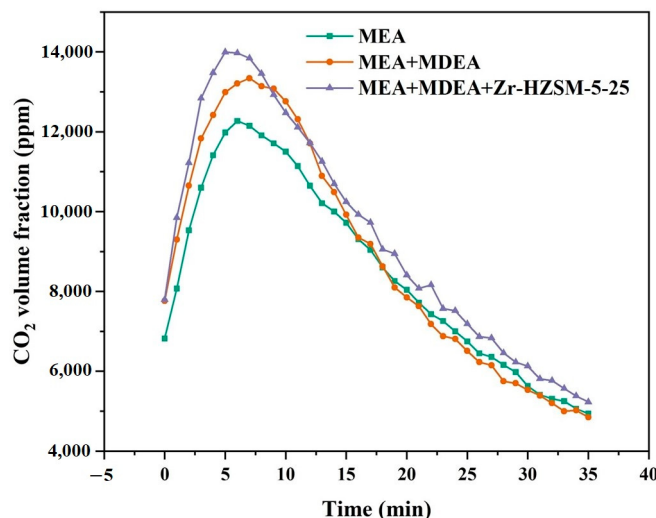


Figure 8. The CO₂ regeneration rate of the mixed amine solution (measured by the equipment shown in Figure 1).

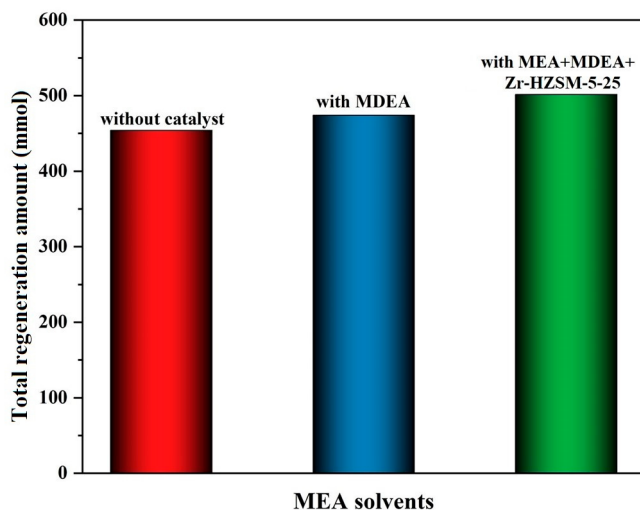


Figure 9. The total CO₂ regeneration amount of the mixed amine solution (measured by the equipment shown in Figure 1).

Additionally, after introducing the catalyst into the MEA + MDEA mixed amine, the regeneration rate increases by only 4.91%. This enhancement is notably less than that of the MEA solution. This discrepancy may be attributed to the fact that the Zr-HZSM-5-25 catalyst primarily facilitates acid-catalyzed reactions, whereas the reaction between MEA and MDEA involves base-catalyzed processes. Consequently, the acidity of the Zr-HZSM-5-25 catalyst may be insufficient to effectively catalyze this base-catalyzed reaction, leading to reduced efficiency. As shown in Table 4, when comparing the average regeneration rates, the Zr-HZSM-5-25 catalyst increases the average regeneration rate in the MEA + MDEA solution by 5.83%. This is similar to the catalytic effect observed with the Zr-HZSM-5-25 catalyst in the MEA solution. This result indicates that the catalytic effect in the MEA + MDEA solution is primarily attributed to the MEA regeneration mechanism, where the acid catalyst provides protons for carbamate decomposition, thus accelerating the CO₂ regeneration rate.

Table 4. The average regeneration rate during the test procedure of the mixed amine solution (measured by the equipment shown in Figure 1).

	MEA	MEA + MDEA	MEA + MDEA + Zr-HZSM-5-25
The average regeneration rate (mmol/min)	12.98	13.54	14.33
The promotion effect (%)	—	4.32	10.42

3.5. The Continuous Absorption and Regeneration Tests

To further investigate the catalyst performance, the bench-scale test is carried out. The absorption efficiency and the regeneration energy consumption are calculated according to Section 3.1.2.

Under cyclic test conditions, the impact of HZSM-5-25 and Zr-HZSM-5-25 solid particles on the regeneration process of MEA-rich solution is studied. The CO₂ regeneration rate is inferred from the CO₂ absorption rate when the system reaches stability. Figure 10 illustrates the variation in system absorption efficiency over 60 min at a regeneration temperature of 105 °C. By integrating this curve and combining it with the CO₂ flow rate in the exhaust gas, the actual CO₂ absorption amount is calculated. The energy consumption for CO₂ generation is shown in Figure 11. The result indicates that, compared to the blank test, both the HZSM-5-25 and Zr-HZSM-5-25 catalysts can accelerate the CO₂ regeneration rate. The HZSM-5-25 catalyst reduces the CO₂ regeneration energy consumption by approximately 4.6%, while the Zr-HZSM-5-25 catalyst lowers the CO₂ regeneration energy consumption by 7.3%. This enhancement is primarily attributed to the improved acidic strength and the increased specific surface area of mesopores and micropores in the modified Zr-HZSM-5-25 catalyst compared to the HZSM-5-25 catalyst. The optimized Zr-HZSM-5-25 catalyst provides more protons for the decomposition of carbamate (reaction (4)) and offers additional nucleation sites for the bubble formation during the MEA solution regeneration at high temperatures. This results in a larger effective surface area at the gas-liquid interface, which enhances the overall mass transfer, accelerates the CO₂ regeneration rates, and reduces the CO₂ regeneration energy consumption. These observations align with the results of Section 3.3.

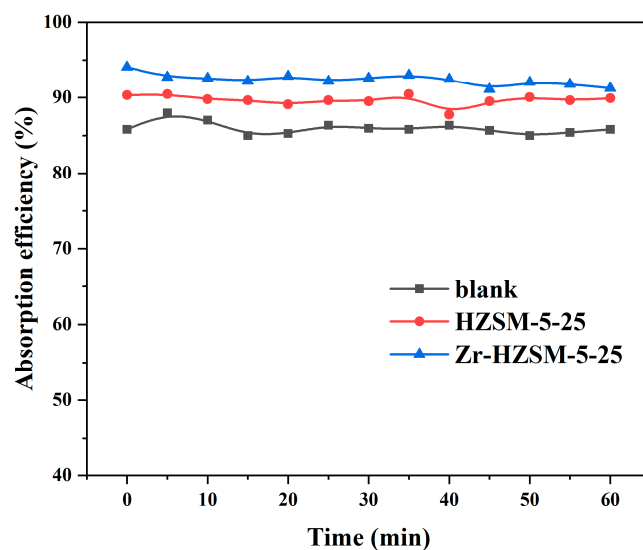


Figure 10. The effect of different catalysts on the absorption efficiency (measured by the equipment shown in Figure 2).

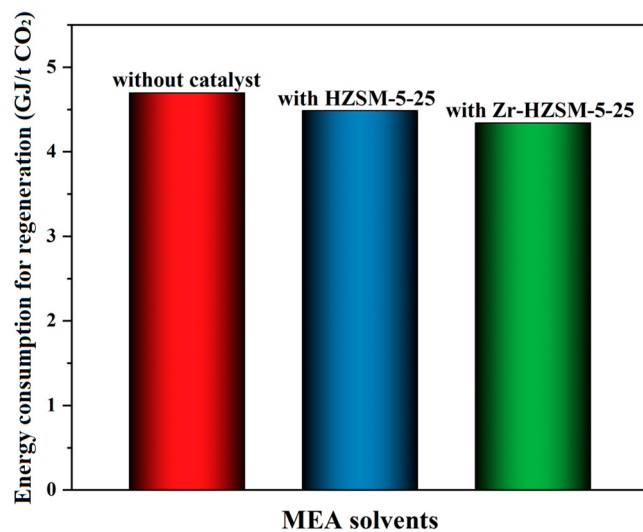


Figure 11. The effect of different catalysts on the regeneration energy consumption (measured by the equipment shown in Figure 2).

4. Conclusions

In this paper, the catalytic effect of several different types of catalysts is investigated. For the MEA regeneration process, the promoting effect of catalysts mainly benefits from the total amount of acid on the surface of catalysts. The Zr-HZSM-5-25 catalyst with the most acid sites effectively increases the CO₂ regeneration peak rate by nearly 8.25%. The HCO₃⁻ generated by the γ-Al₂O₃ in the low-CO₂ loading solution and the CO₂ in solution makes the γ-Al₂O₃ gradually stronger than that of the Zr-HZSM-5-25 catalyst. For the MEA + MDEA mixed amine solution, the reaction of the MDEA with CO₂ produces a large amount of HCO₃⁻, which can simultaneously bind to the proton of the protonated amine and cause heat decomposition into H₂O and CO₂. However, the catalytic effect of the solid acid catalyst is not obvious. This may be because of the possible competition of the MEA reaction with the Zr-HZSM-5-25 catalyst. While the Zr-HZSM-5-25 catalyst shows a better performance in the bench-scale test, it reduces the CO₂ regeneration energy consumption by 7.3%.

Author Contributions: Conceptualization, K.L.; methodology, Y.S.; validation, T.S. and Z.H.; formal analysis, R.Z.; resources, Z.L.; writing—original draft preparation, Y.X.; writing—review and editing, E.H.; supervision, H.Y. All authors have read and agreed to the published version of the manuscript.

Funding: This research was funded by the National Key R&D Program of China, grant numbers 2022YFE0124300 and 2022YFE0208900.

Data Availability Statement: Data are contained within the article.

Conflicts of Interest: The authors declare no conflicts of interest. Authors K.L., Y.S., T.S. and R.Z. are employed by Shanghai Qiyao Environmentally Technology Co., Ltd.; authors K.L., Z.H., Liangjing Luo, Z.L. and H.Y. are employed by Shanghai Marine Diesel Engine Research Institute; author E.H. is employed by JNE SYSTECH Co., Ltd. The authors declare that this research was conducted in the absence of any commercial or financial relationships that could be construed as a potential conflict of interest.

References

- Zhang, S.; Du, M.; Shao, P.; Wang, L.; Ye, J.; Chen, J.; Chen, J. Carbonic Anhydrase Enzyme-MOFs Composite with a Superior Catalytic Performance to Promote CO₂ Absorption into Tertiary Amine Solution. *Environ. Sci. Technol.* **2018**, *52*, 12708–12716. [CrossRef] [PubMed]
- Roufogali, N.; Pyrgakis, K.A.; Kokossis, A.C. Assessment of low-carbon alternative fuels in maritime integrated with CCS on board. In *Computer Aided Chemical Engineering*; Manenti, F., Reklaitis, G.V., Eds.; Elsevier: Amsterdam, The Netherlands, 2024; Volume 53, pp. 1183–1188.

3. Folger, P.F. *Carbon Capture and Sequestration (CCS) in the United States*; Congressional Research Service: Washington, DC, USA, 2017.
4. Tavakoli, S.; Gamlem, G.M.; Kim, D.; Roussanaly, S.; Anantharaman, R.; Yum, K.K.; Valland, A. Exploring the technical feasibility of carbon capture onboard ships. *J. Clean. Prod.* **2024**, *452*, 142032. [[CrossRef](#)]
5. Arvidsson, M.; Heyne, S.; Morandin, M.; Harvey, S. Integration Opportunities for Substitute Natural Gas (SNG) Production in an Industrial Process Plant. *Chem. Eng.* **2012**, *29*, 331–336.
6. Perskin, J.B.; Traum, M.J.; von Hippel, T.; Boetcher, S.K.S. On the feasibility of precompression for direct atmospheric cryogenic carbon capture. *Carbon Capture Sci. Technol.* **2022**, *4*, 100063. [[CrossRef](#)]
7. Wang, Y.; Zhao, L.; Otto, A.; Robinius, M.; Stolten, D. A Review of Post-combustion CO₂ Capture Technologies from Coal-fired Power Plants. *Energy Procedia* **2017**, *114*, 650–665. [[CrossRef](#)]
8. Onarheim, K.; Santos, S.; Kangas, P.; Hankalin, V. Performance and costs of CCS in the pulp and paper industry part 1: Performance of amine-based post-combustion CO₂ capture. *Int. J. Greenh. Gas Control* **2017**, *59*, 58–73. [[CrossRef](#)]
9. Leeson, D.; Mac Dowell, N.; Shah, N.; Petit, C.; Fennell, P.S. A Techno-economic analysis and systematic review of carbon capture and storage (CCS) applied to the iron and steel, cement, oil refining and pulp and paper industries, as well as other high purity sources. *Int. J. Greenh. Gas Control* **2017**, *61*, 71–84. [[CrossRef](#)]
10. Bassani, A.; Bozzano, G.; Pirola, C.; Ranzi, E.; Pierucci, S.; Manenti, F. Low Impact Methanol Production from Sulfur Rich Coal Gasification. *Energy Procedia* **2017**, *105*, 4519–4524. [[CrossRef](#)]
11. Ferrario, D.; Pröll, T.; Stendardo, S.; Lanzini, A. Cost and environmentally efficient design of an absorption-based post-combustion carbon capture unit for industry applications. *Chem. Eng. J.* **2024**, *494*, 152900. [[CrossRef](#)]
12. Ahmed, U.; Kim, C.; Zahid, U.; Lee, C.-J.; Han, C. Integration of IGCC and methane reforming process for power generation with CO₂ capture. *Chem. Eng. Process. Process Intensif.* **2017**, *111*, 14–24. [[CrossRef](#)]
13. Mercure, J.-F.; Mercure, J.-F.; Pollitt, H.; Viñuales, J.E.; Edwards, N.R.; Edwards, N.R.; Holden, P.B.; Chewpreecha, U.; Salas, P.; Sognnaes, I.; et al. Macroeconomic impact of stranded fossil fuel assets. *Nat. Clim. Change* **2018**, *8*, 588–593. [[CrossRef](#)]
14. Narku-Tetteh, J.; Muchan, P.; Saiwan, C.; Supap, T.; Idem, R. Selection of components for formulation of amine blends for post combustion CO₂ capture based on the side chain structure of primary, secondary and tertiary amines. *Chem. Eng. Sci.* **2017**, *170*, 542–560. [[CrossRef](#)]
15. Chen, J.; Luo, W.; Li, H. A review for research on thermodynamics and kinetics of carbon dioxide absorption with organic amines. *Huagong Xuebao/CIESC J.* **2014**, *65*, 12–21. [[CrossRef](#)]
16. Ji, L.; Yu, H.; Yu, B.; Jiang, K.; Grigore, M.; Wang, X.; Zhao, S.; Li, K. Integrated absorption–mineralisation for energy-efficient CO₂ sequestration: Reaction mechanism and feasibility of using fly ash as a feedstock. *Chem. Eng. J.* **2018**, *352*, 151–162. [[CrossRef](#)]
17. Sultan, H.; Quach, T.-Q.; Muhammad, H.A.; Bhatti, U.H.; Lee, Y.D.; Hong, M.G.; Baek, I.H.; Chan, N.S. Advanced post combustion CO₂ capture process—A systematic approach to minimize thermal energy requirement. *Appl. Therm. Eng.* **2021**, *184*, 116285. [[CrossRef](#)]
18. Finotello, A.; Bara, J.E.; Camper, D.; Noble, R.D. Room-Temperature Ionic Liquids: Temperature Dependence of Gas Solubility Selectivity. *Ind. Eng. Chem. Res.* **2008**, *47*, 3453–3459. [[CrossRef](#)]
19. Yu, C.-H.; Huang, C.-H.; Tan, C.-S. A Review of CO₂ Capture by Absorption and Adsorption. *Aerosol Air Qual. Res.* **2012**, *12*, 745–769. [[CrossRef](#)]
20. Sakwattanapong, R.; Aroonwilas, a.; Veawab, A. Behavior of Reboiler Heat Duty for CO₂ Capture Plants Using Regenerable Single and Blended Alkanolamines. *Ind. Eng. Chem. Res.* **2005**, *44*, 4465–4473. [[CrossRef](#)]
21. Shi, H.; Naami, A.; Idem, R.; Tontiwachwuthikul, P. Catalytic and non catalytic solvent regeneration during absorption-based CO₂ capture with single and blended reactive amine solvents. *Int. J. Greenh. Gas Control* **2014**, *26*, 39–50. [[CrossRef](#)]
22. Sun, S.; Lv, Z.; Qiao, Y.; Qin, C.; Xu, S.; Wu, C. Integrated CO₂ capture and utilization with CaO-alone for high purity syngas production. *Carbon Capture Sci. Technol.* **2021**, *1*, 100001. [[CrossRef](#)]
23. Yang, Z.; Shen, Y.; Yang, H.; Yi, H.; Guo, H.; Zhang, X. A review of CO₂ catalytic regeneration research based on MEA solution. *Front. Energy Res.* **2023**, *11*, 1257218. [[CrossRef](#)]
24. Aghel, B.; Janati, S.; Wongwises, S.; Shadloo, M.S. Review on CO₂ capture by blended amine solutions. *Int. J. Greenh. Gas Control* **2022**, *119*, 103715. [[CrossRef](#)]
25. Oh, S.-Y.; Binns, M.; Cho, H.; Kim, J.-K. Energy minimization of MEA-based CO₂ capture process. *Appl. Energy* **2016**, *169*, 353–362. [[CrossRef](#)]
26. Idem, R.; Wilson, M.; Tontiwachwuthikul, P.; Chakma, A.; Veawab, A.; Aroonwilas, A.; Gelowitz, D. Pilot Plant Studies of the CO₂ Capture Performance of Aqueous MEA and Mixed MEA/MDEA Solvents at the University of Regina CO₂ Capture Technology Development Plant and the Boundary Dam CO₂ Capture Demonstration Plant. *Ind. Eng. Chem. Res.* **2006**, *45*, 2414–2420. [[CrossRef](#)]
27. Idem, R.; Shi, H.; Gelowitz, D.; Tontiwachwuthikul, P. Catalytic Method and Apparatus for Separating a Gaseous Component from an Incoming Gas Stream. U.S. Patent US20130108532A1, 2 May 2013.
28. Wang, H.; Tang, S.; Zhong, S.; Liang, B. An investigation of the enhancing effect of solid particle surface on the CO₂ desorption behavior in chemical sorption process with MEA solution. *CIESC J.* **2023**, *74*, 1539–1548.
29. Zhang, X.; Huang, Y.; Yang, J.; Gao, H.; Huang, Y.; Luo, X.; Liang, Z.; Tontiwachwuthikul, P. Amine-based CO₂ capture aided by acid-basic bifunctional catalyst: Advancement of amine regeneration using metal modified MCM-41. *Chem. Eng. J.* **2020**, *383*, 123077. [[CrossRef](#)]

30. Akachuku, A.; Osei, P.A.; Decardi-Nelson, B.; Srisang, W.; Pouryousefi, F.; Ibrahim, H.; Idem, R. Experimental and kinetic study of the catalytic desorption of CO₂ from CO₂-loaded monoethanolamine (MEA) and blended monoethanolamine—Methyl-diethanolamine (MEA-MDEA) solutions. *Energy* **2019**, *179*, 475–489. [[CrossRef](#)]
31. Narku-Tetteh, J.; Afari, D.; Coker, J.; Idem, R. Evaluation of the roles of absorber and desorber catalyst in the heat duty and heat of CO₂ desorption from BEA-AMP and MEA-MDEA solvent blends in a bench scale CO₂ capture pilot plant. *Energy Fuels* **2018**, *32*, 9711–9726. [[CrossRef](#)]
32. Natewong, P.; Prasongthum, N.; Reubroycharoen, P.; Idem, R. Evaluating the CO₂ Capture Performance Using a BEA-AMP Biblend Amine Solvent with Novel High-Performing Absorber and Desorber Catalysts in a Bench-Scale CO₂ Capture Pilot Plant. *Energy Fuels* **2019**, *33*, 3390–3402. [[CrossRef](#)]
33. Caplow, M. Kinetics of carbamate formation and breakdown. *J. Am. Chem. Soc.* **1968**, *90*, 6795–6803. [[CrossRef](#)]
34. Li, T.; Yu, Q.; Barzaghi, F.; Li, C.E.; Che, M.; Zhang, Z.; Zhang, R. Energy efficient catalytic CO₂ desorption: Mechanism, technological progress and perspective. *Carbon Capture Sci. Technol.* **2023**, *6*, 100099. [[CrossRef](#)]
35. Chowdhury, F.A.; Yamada, H.; Higashii, T.; Goto, K.; Onoda, M. CO₂ Capture by Tertiary Amine Absorbents: A Performance Comparison Study. *Ind. Eng. Chem. Res.* **2013**, *52*, 8323–8331. [[CrossRef](#)]
36. Shi, H.; Liang, Z.; Sema, T.; Naami, A.; Usuharatana, P.; Idem, R.; Saiwan, C.; Tontiwachwuthikul, P. Part 5a: Solvent chemistry: NMR analysis and studies for amine–CO₂–H₂O systems with vapor–liquid equilibrium modeling for CO₂ capture processes. *Carbon Manag.* **2012**, *3*, 185–200. [[CrossRef](#)]

Disclaimer/Publisher's Note: The statements, opinions and data contained in all publications are solely those of the individual author(s) and contributor(s) and not of MDPI and/or the editor(s). MDPI and/or the editor(s) disclaim responsibility for any injury to people or property resulting from any ideas, methods, instructions or products referred to in the content.